Part VII
Polar cap phenomena

Thursday afternoon. Session Chair: Janusz Gil

- What physical processes operate in the polar cap region?
  - ⋆ Polar cap phenomena
    - ∗ Individual-pulse modulation properties (drifting subpulses, subpulse "memory", nulling, mode-changing, *etc.*) pertaining to polar cap processes.
    - ∗ Observations of correlated pulse-interpulse emission as they relate to polar cap emission models.
    - ∗ Observation and physical discussion of retardation and aberrational effects in pulsar radiation.

Jim Cordes began the Thursday afternoon session with a comprehensive paper reviewing the observational constraints on pulsar magnetosphere models, entitled, Probing magnetospheres of rotation-driven neutron stars.

https://doi.org/10.1017/S0002731600155283 Published online by Cambridge University Press

PROBING MAGNETOSPHERES OF ROTATION-DRIVEN NEUTRON STARS

JAMES M. CORDES
Astronomy Department, Cornell University and National Astronomy and Ionosphere Center

Abstract

Magnetospheric issues are discussed as they relate to radio intensity variations, spindown, rotational noise, and emission altitudes. Radio fluctuations trace the overall state(s) of the magnetosphere in spite of the fact that $L_{\rm radio} \ll I\Omega\dot{\Omega}$. Five methods for estimating emission altitudes r_e are discussed. Four measure either the transverse width or radial depth of the emission region; assumption of a dipolar field and, in some cases, a radius to frequency mapping, yields estimates for the absolute radius of the emission region. The fifth method (v/c effects in Stokes parameter waveforms) provides direct altitude estimates. Most results suggest that $r_e \lesssim 0.02\ R_{\rm LC}$ at $\nu = 0.4\,$GHz. A radius to frequency mapping appears viable for some but not necessarily all objects. The mapping need not be one-to-one. Prospects are discussed for using simultaneous radio and high energy observations to make further progress in our understanding of magnetospheres.

Intensity fluctuations

The main lesson from 23 years of pulsar observations is that radio fluctuations occur on time scales

$$\delta t \ll P, \qquad \delta t \approx P, \qquad \delta t \gg P, \qquad (1)$$

where P is the spin period. *The magnetosphere is dynamic* on all time scales, particularly those that are much larger than the light travel time across the magnetosphere ($t_{\rm m} \approx R_{\rm LC}/c = P/2\pi$), let alone across various gaps or caps in the magnetosphere. This requires additional (*e.g.* thermal) time constants in the pulsar or that some of the plasma flow be non-relativistic. The radio luminosity is a small fraction of the spindown energy loss:

$$10^{-10} \lesssim L_{\rm radio}/I\Omega\dot{\Omega} \lesssim 10^{-2} \qquad (2)$$

for known pulsars. The causes of radio fluctuations therefore include:

1. Mere fluctuations in the coherence process with little change in the plasma distribution function;

2. Significant changes in the plasma distribution function (density and/or energy);

3. Changes in electric field in regions of particle acceleration that correspond to global changes in the magnetosphere. These items, particularly 2 and 3, are not independent.

Table 1 gives categories of intensity variation, with groupings into $< P$ and $> P$ time scales. For the latter group, variations are further divided into continuous and discontinuous variations.

Examples of intensity variations are given in figure 1. Intense *subpulse* and *micropulse* variations are evident (figure 1a) along with the general extreme variability from pulse to pulse. Microstructure is prone to *quasiperiodicity* (Boriakoff 1976, Cordes 1976a, Kardeshev *et al.* 1978) with periods $0.1\,{\rm ms} \lesssim P_\mu \lesssim 4\,{\rm ms}$ (to be discussed more later). Micropulses (figure 1b)

show yet finer structure down to the inverse receiver bandwidth ($0.8\,\mu$s) (Hankins and Boriakoff 1978). The finest structure is not real as it reflects *noise* resulting from *incoherent processes* in the pulsar magnetosphere (Hankins and Boriakoff 1978, Rickett 1975, Cordes 1976a). The microstructure is a modulation of a noise process whose statistics are complex Gaussian in the electric field and, therefore, are one-sided exponential in the intensity. The short time-scale statistics of pulsar signals are, therefore, no different from those of incoherent synchrotron sources (*e.g.* active galactic nuclei). *Pulse nulling* and *drifting subpulses* are exemplified in figure 1c for PSR 1944+17, which shows more null (55%) than 'on' pulses. *Waveform mode changes* (Bartel *et al.* 1982) (figure 1d), like nulling, occur suddenly with broadband transitions from one state to another in less than one spin period. These latter phenomena provide strong evidence that the overall state of the magnetosphere changes suddenly when mode changes or nulling occur. Several pulsars show a preference for *quantized drift rates* (Wright and Fowler 1981) where the subpulse drift rate varies between (often three) values or the average pulse shape can take on two or three forms.

The best constraint on the null transition time is from study of PSR 1944+17 (Deich *et al.* 1986).

https://doi.org/10.1017/S0002731600155283 Published online by Cambridge University Press

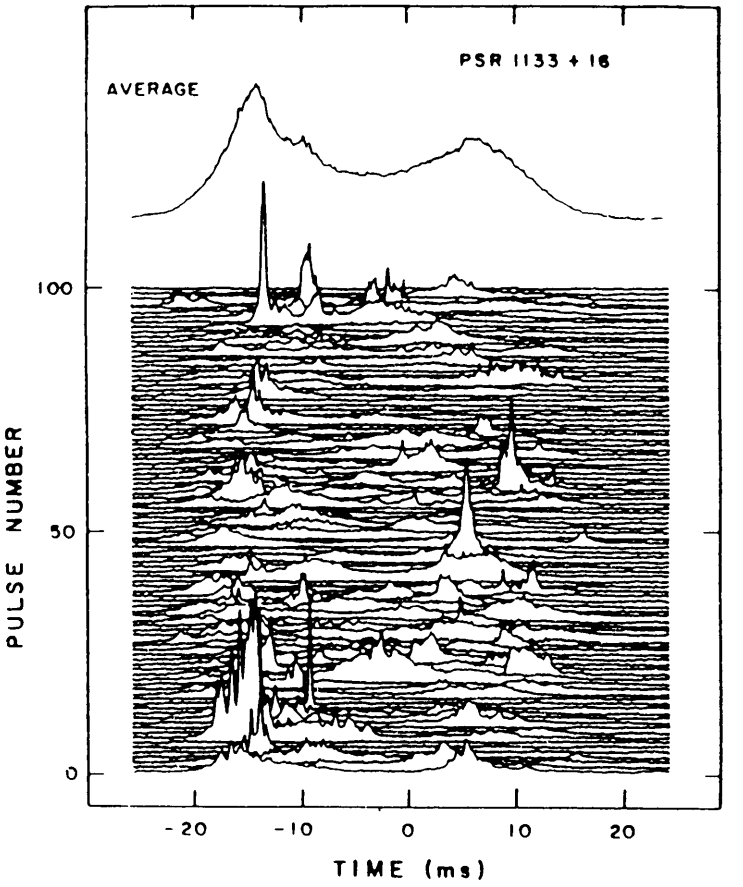

Figure 1a Sequence of pulses from PSR 1133+16 obtained from the Arecibo Observatory.

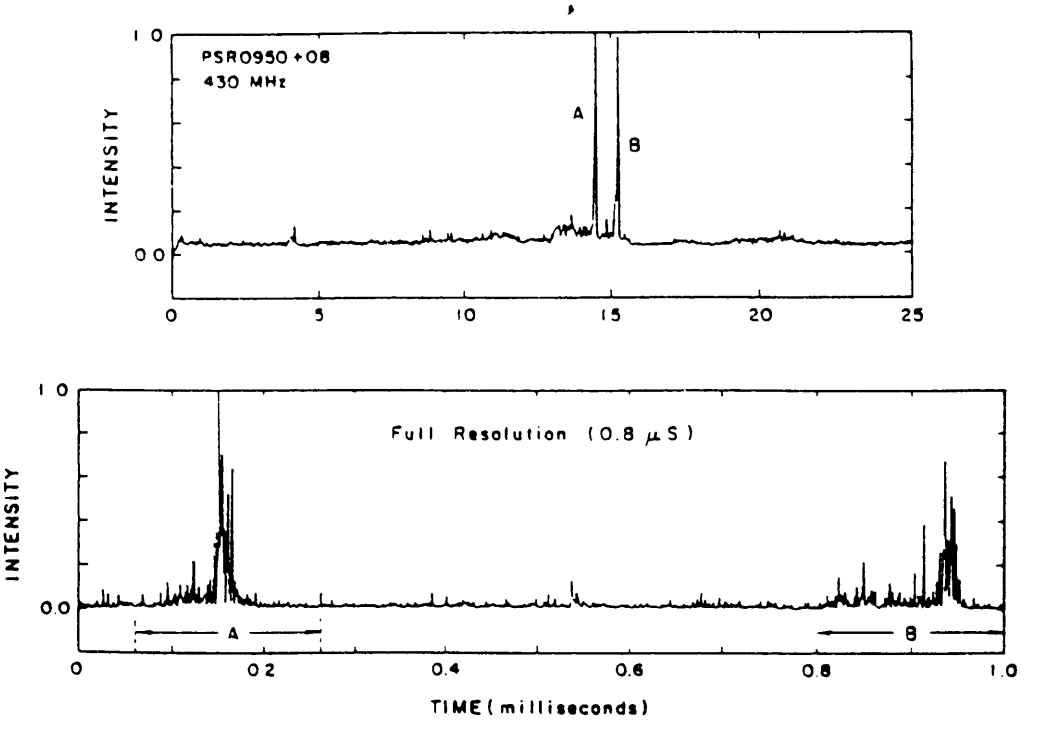

Figure 1b A single pulse from PSR 0950+08 showing two intense micropulses.

The absence of intensity discontinuities places a lower bound on the transition time of 2 ms while the ratio of pulse strengths before and after a null gives an upper bound of 30 ms. Nulls seem to occur by the cessation of subpulses rather than by a process that is independent of subpulse modulations.

https://doi.org/10.1017/S0002731600155283 Published online by Cambridge University Press

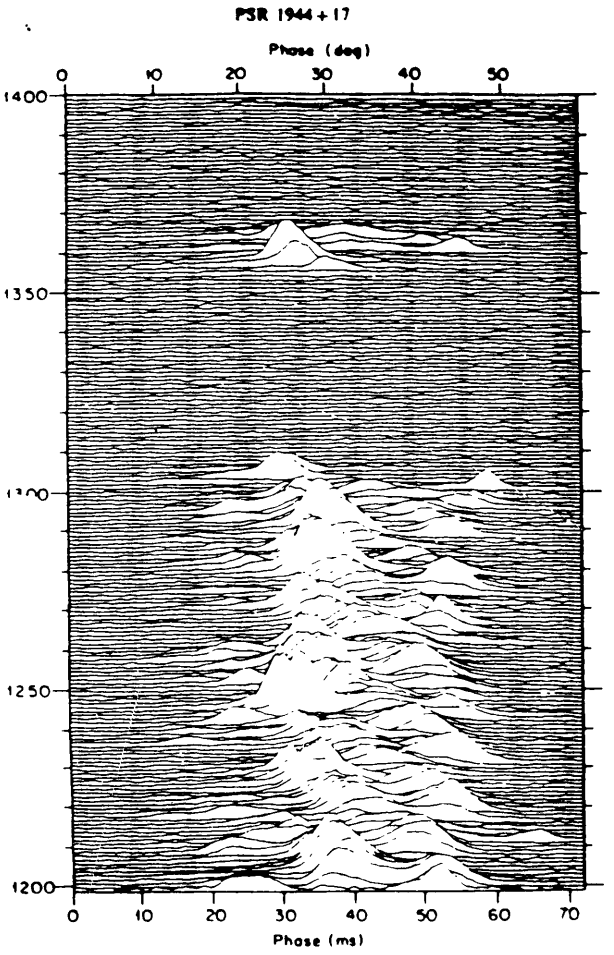

Figure 1c Pulse sequence from PSR 1944+17 showing nulls and drifting subpulses (Deich *et al.* 1986).

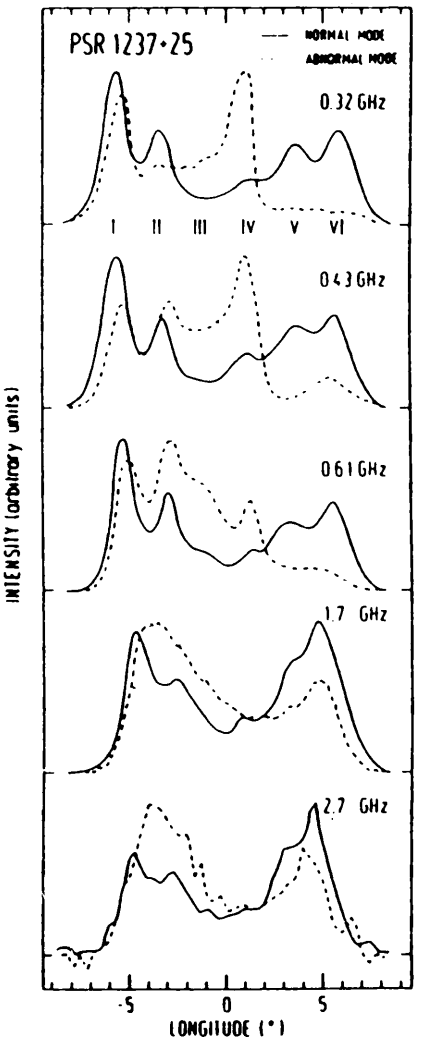

Figure 1d Average waveforms from PSR 1237+25 for 'normal' and 'abnormal' modes (Bartel *et al.* 1982).

Both the null transition time and subpulse duration may therefore derive from the depth and/or width of the column of emitting plasma in the open field line region.

Intertwined null and drift phenomena are manifest in PSR 0809+74 which shows that the subpulse drift path recovers from a null according to the length of the null (Lyne and Ashworth 1983). The physical entity that produces subpulses therefore survives a null and its location and motion depend on the null duration. Proposals for subpulse drift include $\boldsymbol{E} \times \boldsymbol{B}$ drifts or low frequency drift waves. Large fractional changes in drift rate require, in either model, large changes in $\boldsymbol{E}$ or in plasma density or energy. Current thinking therefore implicates the entire magnetosphere as the 'cause' of changes in intensity fluctuation patterns.

Microstructure often shows a 'quasiperiodicity' by which it is meant that the spacing between micropulses P_μ takes on preferred values and that, in some single pulses, strings of $\lesssim 10$ micropulses are seen. The spacing P_μ can change from one subpulse to the next and from one pulse period to the next. Histograms of P_μ show broad distributions covering 10:1 ranges.

Polarization fluctuations

Average Stokes parameter waveforms show (Manchester and Taylor 1977): (*i*) as much as 100% linear polarization; (*ii*) generally small (~5%) but as much as ~60% circular polarization; (*iii*) a variation of position angle $\psi(\phi)$ that is often consistent with that expected from the projection of dipolar magnetic field lines (see below); (*iv*) discontinuities in $\psi(\phi)$ at some pulse phases ϕ by $\sim \pm\pi/2$; (*v*) changes in sense of circular polarization in the centroid regions of some pulses (Radhakrishnan and Rankin 1990).

Individual pulses show similar phenomena, with the orthogonal modes manifested as switching in $\psi(\phi)$ both within single pulses and from pulse to pulse (Backer and Rankin 1980). Polarization sig-

https://doi.org/10.1017/S0002731600155283 Published online by Cambridge University Press

Table 1 Pulsar intensity variations

Kind	Description	Δt	Properties
Intrapulse	*i.* micropulse	$1\,\mu s$ – few ms	quasiperiodic: $0.1\,\text{ms} < P_\mu < 4\,\text{ms}$; prominent for $\nu < 1\,\text{GHz}$ and small $\dot{P}$.
	ii. subpulse	1 ms – 100 ms	width, spacing $\propto \nu^x$, $-0.2 < x < 0.5$; drifting subpulses for small $\dot{P}$.
Pulse to pulse			
a. continuous			
	i. subpulse drift	$P_2 \approx 5 - 20\,\text{ms}$ $P_3 \approx 3 - 1000P$	drift rate P_2/P_3; nonlinear drift paths; quantized drift rates.
	ii. quasiperiods	$\approx P_3$	
	iii. aperiodic	P to years	bursts, trends, white noise.
b. discontinuous			
	i. nulling	durations $\approx 1 = 5000P$; rise/fall times $< P$.	no radio emission; correlated with $P\dot{P}^{-x}$, $2 < x < 3$.
	ii. waveform mode change	"	broadband; changes in pulse component heights and spacings.
	iii. drift rate changes	"	quantized drift rates.

natures are sometimes reported to "follow" drifting subpulses (Taylor *et al.* 1971) but this appears to be due to mode switching that tends to occur on the periphery of subpulses. Most, if not all, polarization fluctuations (and depolarization) may be accounted for by the geometrical rotation in item (*iii*) above combined with orthogonal modes and the overlap of core and conal components.

Relationship of intensity variations to rotational activity?

The intensity phenomena we have discussed appear only in some objects and, then, to varying degree. There is segregation in the P–$\dot{P}$ plane of objects that show mode changing and nulling. Nulling is prevalent in objects displaying conal emission but is absent in objects that show only core emission (Rankin 1986). However, there is no obvious relation to proximity to the 'death line' where, perhaps, radio pulsars abruptly turn off. Contrariwise, the death line may be only a statistical outer envelope, with nulling indeed being the path by which objects begin terminating their emission. This latter view is supported by the appearance of the pulsar period distribution, dN/dP. In going from small to large P, dN/dP rises as it would for a population with constant birthrate without death; but at $P \approx 0.4\,\text{s}$ it begins to level off. Consequently, some objects must terminate their emission or become undetectable for P as small as 0.4 s.

Mode changes tend to be found in objects with low to modest $\dot{P}$ (Rankin 1983a) while microstructure and drifting subpulses tend to be found in low $\dot{P}$ objects (Rankin 1986, Cordes, Weisberg, and

https://doi.org/10.1017/S0002731600155283 Published online by Cambridge University Press

Hankins 1990).

The possible relationship of intensity phenomena to *rotational ('timing') noise* should also be considered. There is no obvious correlation of nulling with rotational noise (Cordes and Helfand 1980), while mode changes tend to occur in objects with small timing noise (Wright and Fowler 1981). Timing noise is itself correlated with $\dot{P}$ and is most likely due to rotational activity *internal* to the neutron star (Cordes and Helfand 1980, Cordes and Downs 1985). Therefore, any possible relation of magnetospheric phenomena to rotational noise may be coincidental, rather than causal *via* $\dot{P}$, which is related to the magnetic field strength at the light cylinder and to the torque, which alters the differential rotation between the superfluid neutrons and the outer crust.

If microstructure or subpulse quasiperiodicities are due to neutron-star oscillations (Boriakoff 1976, Van Horn 1980), one must question how the low Q intensity variations are induced by high Q stellar oscillations. Stellar oscillations are damped on time scales $\ll P/2\dot{P}$ so the core/crust differential rotation is a natural source of free energy, possibly tapped by rotational noise. Why, then, do quasiperiodicities appear in objects with the *smallest* rotation noise? Perhaps it is only in such objects that quasiperiodicities can be recognized: excessive rotation noise may produce *too complex* magnetospheric activity, as suggested by studies of mode-mode coupling of torsional oscillations (Nelson and Wasserman 1989).

Altitudes of radio emission regions

There are 5 methods by which emission altitudes may be estimated.

1. The period-pulse width relation.

The open field-line region produces radio beams of angular radius

$$\rho = \frac{3}{2}\left(\frac{r_e}{R_{LC}}\right)^{1/2} \approx 2.^{\circ}49 P^{-1/2}\left(\frac{r_e}{R}\right)^{1/2}\left(\frac{R}{10\ \mathrm{km}}\right)^{1/2} \quad (3)$$

for $\rho \ll 1$, where $R_{LC} \equiv c/\Omega$, r_e is the radius of the emission region, and R is the neutron star radius. Observed pulse widths, if related to the extent of the open field-line region, would be

$$\hat{W} = \frac{2}{\sin\alpha}\left(\rho^2 - \sigma^2\right)^{1/2}, \quad (4)$$

where $\alpha = \cos^{-1}\hat{\Omega}\cdot\hat{m}$ and $\sigma = \cos^{-1}\hat{n}\cdot\hat{m}$ with $\hat{\Omega}, \hat{m}, \hat{n}$ being unit vectors along the spin axis, magnetic moment, and line of sight (from pulsar to observer). Comparison of $\hat{W}$ to observed pulse widths W suggests $r_e \approx 10$ to $100\ R$ for conal components and $r_e \approx R$ for core components. The general widening of waveforms with decreasing frequency necessarily implies (in this model) that lower frequencies arise from larger r_e, *i.e., a radius to frequency mapping.* When observed pulse widths are plotted against P, a lower envelope $W_\ell = W_1\ P^{-1/2}$ is found (with W_1 different for core and cone components) (Rankin 1990). Objects that fall *on* the envelope are predominantly pulsars with interpulses, suggesting that $\sin\alpha = 1$, $\sigma = 0$ and that $r_e =$ constant for most objects. It is surprising that some objects do not fall below the envelope, since $\hat{W} \to 0$ as $\sigma \to \rho$. Perhaps (Blaskiewicz, Cordes, and Wasserman 1991) the radial depth of the emission region or Lorentz factor determines the minimum pulse width rather than ρ.

2. Arrival time (TOA) *vs.* frequency.

Departures from $TOA(\nu) \propto \nu^{-2}$ (the cold plasma dispersion law in the interstellar medium) may be interpreted as delays produced in the magnetosphere (Cordes 1978, Matese and Whitmire 1980, Kardeshev *et al.* 1982, Phillips and Wolszczan 1990) so long as additional interstellar delays (such as those due to angle-of-arrival variations) may be neglected. Recent work suggests that interstellar delays not $\propto \nu^{-2}$ are negligible (Cordes *et al.* 1990). Magnetospheric contributions may represent a combination of ν dependent propagation (*e.g.* refraction), a variation of emission location (*e.g.* r_e or in magnetic polar coordinates) with frequency, possibly combined with distortion of $\boldsymbol{B}$ from a dipolar form at low or high altitudes. Upper bounds on departures $\Delta t(\Delta\nu)$ from a ν^{-2} law for two frequencies separated by $\Delta\nu$ suggest bounds on the radial difference

$$\Delta r_e < c\Delta t(\Delta\nu)/2 \approx 150\ \mathrm{km}\ \Delta t(\Delta\nu)_{\mathrm{ms}}.$$

The factor of 1/2 accounts for contributions from both aberration and retardation; field line sweep-back may cancel some of the anticipated delay, thereby softening the upper limit. Assumption of a dipolar field combined with a radius to frequency mapping allows conversion of the radial depth into a limit on the absolute emission radius $r_e(\nu)$. Table 2 gives all limits obtained to date, indicating that for $\nu \approx 0.1$ GHz, $r_e \lesssim 0.03 R_{LC}$.

3. v/c effects in intensity and polarization waveforms.

Unlike the Radhakrishnan and Cooke (1969) model that relates polarization angles to projected mag-

https://doi.org/10.1017/S0002731600155283 Published online by Cambridge University Press

Table 2 Emission altitudes from TOA(ν)

PSR	ν_{min} (MHz)	ν_{max} (MHz)	$\Delta r_e = r_e(\nu_{min}) - r_e(\nu_{max})$ (km)	$r_e(\nu_{min})/R_{LC}$	Ref
0525+21	112	613	$\lesssim$3000	$\lesssim$0.03	1
0823+26	47	4800	$\lesssim$210	$\lesssim$0.01	5
0834+06	47	1408	$\lesssim$200	$\lesssim$0.003	5
0919+06	47	4800	$\lesssim$200	$\lesssim$0.01	5
0950+08	40	430	$\lesssim$1000	$\lesssim$0.08	1
	111	318	60 ± 30	0.01	2
	47	4800	$\lesssim$210	$\lesssim$0.02	5
1133+16	40	1400	$\lesssim$500	$\lesssim$0.01	1
	102	970	450 ± 150	0.007-0.03	3
	52	4800	$\lesssim$150	0.003	5
1604−00	47	430	$\lesssim$150	0.007	5
1937+214	318	1400	$\lesssim$2	—[a]	4

References: (1) Cordes 1978; (2) Rickett and Cordes 1981; (3) Kardashev *et al.* 1982; (4) Cordes and Stinebring 1983; (5) Phillips and Wolszczan 1990

Note a: The waveforms from the first millisecond pulsar cannot be interpreted in terms of an open field line region model with radius to frequency mapping.

netic field lines, the actual polarization results from particle trajectories determined by *corotation* as well as by B. Corotation alters the radius of curvature of particle trajectories across the pulse, thereby breaking the symmetry of the dipolar field. For emission at r_e, the additional $\Omega \times r_{em}$ effects include (Blaskiewicz, Cordes, and Wasserman 1991): (*i.*) aberration of the intensity waveform to earlier time by $\delta t_I \approx -r_e/c$; (*ii.*) shift of the polarization position angle curve to later time by $\delta t_\psi \approx +3r_e/c$; (*iii.*) A total shift between the centroids of the I and ψ waveforms of $\delta t_T \approx 4r_e/c$. (*iv.*) An increase in intensity ratio R_{12} of the first to second component (in conal double waveforms) to $R_{12} > 1$ by an amount that depends on r_e.

Thus, v/c effects can yield emission radii *without* assumption of a radius to frequency mapping and allow assessment of the role of curvature of particles' trajectories in determining the intensity waveform (whether in a curvature radiation or plasma maser model).

Results on 23 objects indicate (Blaskiewicz, Cordes, and Wasserman 1991) that for 12 conal doubles, $\delta t_T > 0$ for 6 objects, $\delta t_T \approx 0$ for 5 objects, and $\delta t_T < 0$ for one object. For 8 core/single objects these numbers are 5, 2, and 1 while for 3 unclassifiable ('complex') objects they are 2, 1, and 0. Emission altitudes are equal to or limited to 100 to 1000 km, in general agreement with the period-pulse width relation. Moreover, in 88 conal objects studied by Lyne and Manchester 53 have $R_{12} > 1$ while 24 have $R_{12} < 1$. It also appears possible that the 'one sided conal' objects are simply extreme examples where $r_e/R_{LC} \approx 0.1$.

4. Interstellar scintillation (ISS) constraints on transverse separations of emission regions.

Curvature of magnetic field lines and relativistic beaming require that emission regions of different pulse components *necessarily* be spatially separated at their respective emission times. The isoplanatic or critical angle for ISS is typically $\lesssim 0.1\,\mu$arc sec, sufficiently small to resolve transverse separations in pulsar magnetospheres. Application of ISS to this problem has been done under the situations of (*i.*) 'normal' diffractive scintillation; and (*ii.*) episodes of multiple imaging when dramatic fringes are seen in dynamic spectra, $I(\nu, t)$.

ISS methods rely on computation of correlation functions of dynamic spectra. Consider $I(\phi, t)$ = intensity as a function of pulse phase ϕ and time t and $I_{1,2} \equiv I(\phi_{1,2}, t)$ is the intensity of pulse components 1 and 2. Let the positions of the emission

https://doi.org/10.1017/S0002731600155283 Published online by Cambridge University Press

regions 1 and 2 be

$$\boldsymbol{X}_{1,2} = \boldsymbol{X}_{s_{1,2}} + \boldsymbol{V}_\perp t \qquad (5)$$

with $\boldsymbol{X}_s$ being the transverse position vector of the source relative to the line pointing from the center of the star toward the observer and $\boldsymbol{V}_\perp$ the transverse velocity of the pulsar. Then the intensity covariance is

$$\begin{aligned}\Gamma(\tau) &\equiv \langle \delta I_1(t)\delta I_2(t+\tau)\rangle \\ &= \exp\left\{-\left[\left(\frac{\Delta X_x}{\ell_x}\right)^2+\left(\frac{\Delta X_y}{\ell_y}\right)^2\right]^{5/6}\right\},\end{aligned}$$

where $\Delta\boldsymbol{X} \equiv |\boldsymbol{X}_{s_2} - \boldsymbol{X}_{s_1} + \boldsymbol{V}_\perp(\tau+\delta t)|$ and $\delta t \equiv (\phi_2 - \phi_1)P \equiv P\Delta\phi$ is the time separation of pulse components. The characteristic lengths of the diffraction pattern are $\ell_{x,y}$; an isotropic scattering medium would give $\ell_x = \ell_y$. The 5/6 exponent arises from assumption of a Kolmogorov spectrum for interstellar turbulence.

Using epochs of normal ISS (Cordes, Weisberg, and Boriakoff 1983), it has been shown that $\Gamma(\tau = 0) = 1 \pm 0.01$, yielding an upper bound on ΔX_s and, assuming a dipolar field which implies $\Delta X_s = r_e\Delta\phi/3$, upper bounds on r_e. Results at 0.43 GHz for pulsars 0525+21 and 1133+16 give $r_e \lesssim 0.06R_{LC}$ and $r_e \lesssim 0.5R_{LC}$, respectively. An alternative approach involves computation of the lag τ_{max} at which the maximum of Γ occurs. For isotropic scattering this yields $\Delta X_s = -V_\perp(\tau_{max} + \delta t)/\cos\Delta\chi$ where $\cos\Delta\chi \equiv \hat{\boldsymbol{\Delta X}}_s \cdot \hat{\boldsymbol{V}}_\perp$. Assuming $\cos\Delta\chi \approx 1$, this yields $r_e \approx 0.08R_{LC}$ for PSR 1133+16 at 0.1 GHz.

For transient intervals, pulsar images are evidently split into multiple images, beating of which produces fringes in dynamic spectra. The fringes are analogous to those from a conventional interferometer and correspond to a baseline ≈ 1 AU (Wolszczan and Cordes 1987). A phase shift of the fringes is expected in comparing two emission regions separated by $\boldsymbol{\Delta X}_s$. The fringe phase shift is (Cordes and Wolszczan 1988)

$$\delta\Phi = \boldsymbol{\Delta X}_s \cdot \boldsymbol{\nabla}_\perp\Phi = \frac{2\pi\,\Delta X_s\cos(\chi_{\Delta x} - \chi_\nabla)}{V_\perp\, P_t\cos(\chi_v - \chi_\nabla)},$$

where χ_x, χ_v, and χ_∇ are position angles of the emission region difference vector, pulsar space velocity, and lens gradient, respectively and P_t is the spacing of fringes in time.

Results on PSR 1237+25 at 0.43 GHz (Wolszczan and Cordes 1987) and PSR 1919+21 (Kuz'min 1992) at 0.1 GHz indicate that $r_e \approx R_{LC}$ if the cosines ≈ 1. These radii are much larger than other estimates and suggest that fringes are recognized only at special times, *e.g.*, when $\cos(\chi_v - \chi_\nabla) \ll 1$.

5. Visibility measurements using space VLBI

The AU-sized baseline necessary for resolving pulsar magnetospheres may be achievable with one of the proposed orbits for RADIO ASTRON (L. Gurvits, private communication). In concert with large ground-based antennas, VLBI at 327 MHz of strong nearby pulsars may yield direct determinations of the transverse separations of emission regions, as in method (4). Space VLBI observations will necessarily be very messy because of amplitude and phase fluctuations induced by interstellar and interplanetary scattering. Nonetheless, *differential* measurements between pulse components appear feasible.

Probing the nature of radio intensity variations

The Crab pulsar presents an important possibility for testing whether radio fluctuations are mere variations in a coherence process that requires 'fine tuning' or that they reflect significant variations in the plasma outflow. The average pulse shape from the Crab pulsar consists of a mainpulse and interpulse that arrive simultaneously to within ~ 1 ms at all wavelengths from the radio to γ-ray. The mainpulse and interpulse originate from large altitude in order that the γ-rays be able to escape the magnetosphere. A radio 'precursor' to the mainpulse may correspond to low altitude emission seen from other objects.

Unlike other pulsars, the Crab displays 'giant' radio pulses from the main and interpulse but *not* the precursor, with the mainpulse favored by 3:1 (Hankins 1990). The amplitude distribution is power law such that pulses with amplitudes 100 times larger than the mean occur $\sim 1\,\text{hour}^{-1}$. Optical variations, on the other hand, are less than 1% (Heygi, Novick, and Thaddeus 1971).

It is conceivable that radio pulses fluctuate because there are variations in pair production that also would cause (anticorrelated?) γ-ray variations. Simultaneous radio and γ-ray observations (with the Gamma Ray Observatory) can establish any such correlation or, like the optical, show γ-ray steadiness. The outcome of this observation, and others that can be imagined, will yield robust conclusions about fluctuations in plasma flow in pulsar magnetospheres.

https://doi.org/10.1017/S0002731600155283 Published online by Cambridge University Press

Discussion

The phenomena and techniques I have discussed are not intended to comprise a complete list. Rather they represent a personal choice (within the confines of the Proceedings page limit) of those areas where recent and future progress appear significant and feasible.

Future work should include:

1. More work on the interstellar scintillation method for resolving pulsar magnetospheres, in new observations and better theory for inversion of the data into constraints on magnetospheric structure.

2. Ground breaking work on joint radio and high energy observations with space observatories such as GRO, ROSAT and AXAF. *Any* correlation, anticorrelation, or lack of correlation will provide useful information about particle flow. Moreover, as J. Arons has mentioned, X-ray observations of radio pulsars may show evidence for polar cap heating fluctuations.

3. More work on the possible link, if any, of observed quasi-periodicities and neutron star oscillations.

Conceptually we should sharpen our questions about the nature of the emission mechanism. For instance, what do we mean by there being two emission mechanisms? Is this the *same particles* emitting *via* two different processes or *different particle* populations emitting *via* the same process?

In addition, we must decide at what point we have come to understand radio pulsar emission. For single objects, individual pulses appear to be 'weather' that average into a waveform 'climate'. Why is the climate different from pulsar to pulsar? Are all neutron stars the same or do the distinguishing characteristics of each object depend on the particular evolutionary history and composition?

Acknowledgments: This research was supported by the National Astronomy and Ionosphere Center, which operates the Arecibo Observatory under contract with the National Science Foundation. Support was also received from the NSF under grant AST 85-20530 and from NASA under grant NAG5-1247.